Communication

Effect of Spin-Ladder Topology on 2D Charge Ordering: Toward New Spin-Antiferroelectric Transitions

Bangbo Yan, Marilyn M. Olmstead, and Paul A. Maggard

J. Am. Chem. Soc., **2007**, 129 (42), 12646-12647• DOI: 10.1021/ja0754709 • Publication Date (Web): 29 September 2007

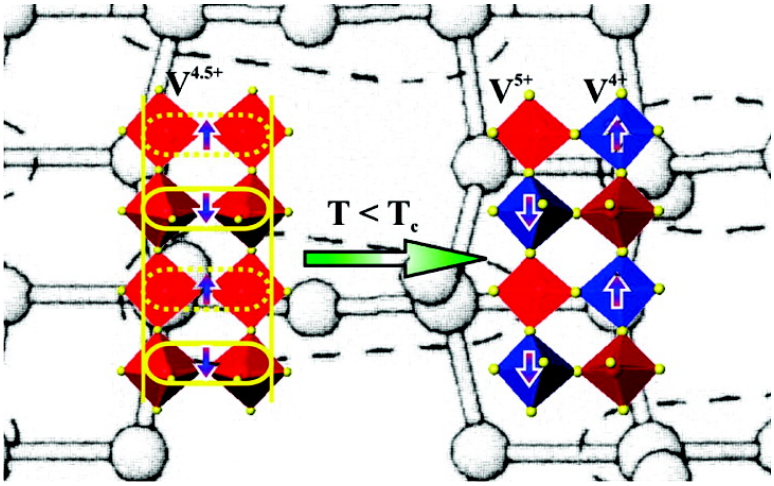

More About This Article

Additional resources and features associated with this article are available within the HTML version:

- Supporting Information
- Links to the 5 articles that cite this article, as of the time of this article download
- Access to high resolution figures
- Links to articles and content related to this article
- Copyright permission to reproduce figures and/or text from this article

View the Full Text HTML

J|A|C|S
COMMUNICATIONS

Published on Web 09/29/2007

Effect of Spin-Ladder Topology on 2D Charge Ordering: Toward New Spin-Antiferroelectric Transitions

Bangbo Yan,[†] Marilyn M. Olmstead,[‡] and Paul A. Maggard*,[†]

Department of Chemistry, North Carolina State University, Raleigh, North Carolina 27695, and Department of Chemistry, University of California at Davis, Davis, California 95616

Received July 22, 2007; E-mail: paul_maggard@ncsu.edu

Solid-state magnetic phase transitions are the focus of intense research efforts for their singular insights into strongly correlated electrons.[1] Layered vanadates have attracted considerable interest as low-dimensional quantum spin ($S = 1/2$) systems and feature a remarkable number of examples of spin dimers, ladders, and other extended spin systems with spin-gapped and/or charge-ordered states.[2,3] Further, their spin-exchange constants can rival those found in layered superconducting cuprates.[4−6] However, the ability to tune or expand upon their magnetic properties is often hindered by the absence of functionality or flexibility to target more optimal structural modifications. Described herein is a surprising new type of charge ordering that emerges coupled to a spin-gapped state in M(pyz)V_4O_{10} (M = Zn, Co; pyz = pyrazine), which demonstrates the remarkable potential of using metal-organic layers in the pursuit of advanced magnetic properties.

The discovery in ά-NaV_2O_5 of a magnetic transition to a spin-gapped ground state has been a prominent but controversial example of a low-temperature phase transition that was initially classified as only the second known spin-Peierl's ladder system.[7,8] Though, recent investigations have revealed this transition occurs together with a unique charge ordering and is more accurately described as a spin-superantiferroelectric (spin-SAF) transition.[9−12] In this model, the unpaired electrons on the VO_5 tetragonal pyramids both charge disproportionate ($2V^{4.5+} \rightarrow V^{4+} + V^{5+}$) into a 2D-ordered zigzag pattern at low temperatures, and as well, a spin gap opens. Theoretical models suggest an intriguing interplay of spin and charge degrees of freedom,[12−14] but further insights are limited by the singularity of its existence. Moreover, the attempted low-temperature structural determinations of ά-NaV_2O_5 are hindered by its many different superstructures, manifested as a "devil's staircase"-type behavior with temperature or pressure.[15] Presented herein is low-temperature single-crystal X-ray evidence for the first known hybrid oxide/organic solid to exhibit the new proposed spin-SAF transition, but with the incorporation of metal-organic layers that yield both a distinctly new and better characterized charge ordering in Zn(pyz)V_4O_{10} and its complete suppression in the isostructural Co(pyz)V_4O_{10}.

The synthesis of M(pyz)V_4O_{10} (M = Zn, Co) was performed according to the reported procedures, with the crystals exhibiting a transition to a nonmagnetic singlet ground state at $T_c \sim 22$ K for M = Zn.[16] To probe the origins of this transition, a black-colored crystal of each was selected for a single-crystal X-ray analysis at $T = 12$ and 10 K for M = Co and Zn, respectively.[17] The lattice parameters and space group for Co(pyz)V_4O_{10} matched well with the higher temperature structure determination,[16] within space group *Cmcm* and $a = 14.3108(4)$ Å, $b = 6.9979(9)$ Å, and $c = 11.4476(7)$ Å. However, Zn(pyz)V_4O_{10} showed a clear lowering of symmetry to $C222_1$ with $a = 14.438(1)$ Å, $b = 6.9788(5)$ Å, and $c = 11.4743(5)$ Å. The unit-cell volume of Co(pyz)V_4O_{10} decreases

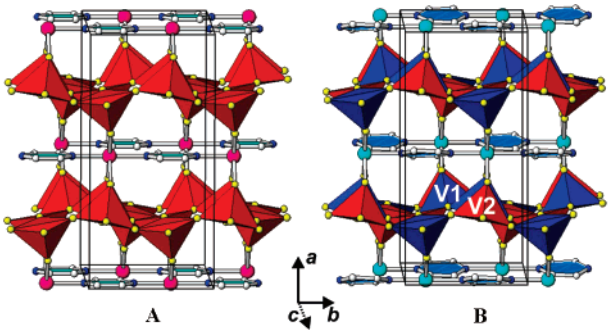

Figure 1. Unit-cell views of the low-temperature structures of M(pyz)-V_4O_{10} for (A) M = Co and (B) M = Zn. Red and blue polyhedra are VO_5, purple = Co, light blue = Zn, yellow = O.

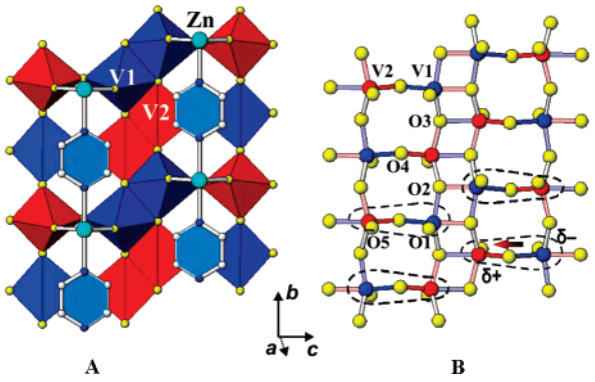

Figure 2. The charge-ordered vanadate layer of Zn(pyz)V_4O_{10}, drawn using (A) polyhedra (V^{4+}, blue; V^{5+}, red) and Zn(pyz)$^{2+}$ chains, and in a (B) ball-and-stick structure with atom labels.

(~0.4%) owing entirely to a contraction of the *c*-axis dimension, while the unit cell volume for Zn(pyz)V_4O_{10} increases (~0.17%) owing to an expansion of the *b*- and *c*-axes but contraction of the *a*-axis dimension.

Unit-cell views of both hybrids are drawn in Figure 1, with Co(pyz)V_4O_{10} (panel A) retaining nearly an identical structure and atomic coordinates as described previously.[16] Generally, this structure is comprised of alternating $V_4O_{10}^{2-}$ layers and M(pyz)$^{2+}$ layers of chains. Above the transition temperature, and for M = Co here, the $V_4O_{10}^{2-}$ layers are formed from the edge- and corner-sharing of one symmetry-unique VO_5 square pyramid centered by $V^{4.5+}$, on average. Shown in Figure 2A, the late transition metals are coordinated to two bridging pyrazine ligands and also to the neighboring vanadate layers above and below. Significantly, this bonding by the metal-organic layers affects the alignment of apical O atoms in the vanadate layers, as well as the resulting charge-ordered state, compared to that in ά-NaV_2O_5.

The low-temperature structure of Zn(pyz)V_4O_{10}, by contrast, contains significant atomic displacements away from the parent structure that result in a splitting of vanadium atoms into two

[†] North Carolina State University.
[‡] University of California at Davis.

10.1021/ja0754709 CCC: $37.00

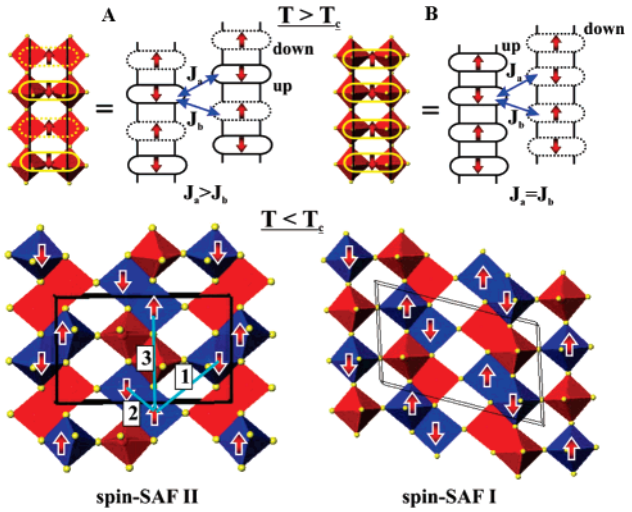

Figure 3. The vanadate intra- and inter-ladder topologies and spin-exchange interactions in $Zn(pyz)V_4O_{10}$ (A) and ά-NaV_2O_5 (B), leading to the charge-ordered structures at $T < T_c$ (bottom).

symmetry-inequivalent positions, as shown in all figures as the red and blue polyhedra. The net atomic displacements around V2 primarily produce a shortening of the intralayer V2−O4 distance (1.711(4) Å; $\Delta_d = -0.102$ Å) and a relatively smaller increase of the V2−O3 distance (2.050(3) Å; $\Delta_d = 0.053$ Å), Figure 2B. The overall effect on the V1 coordination environment is roughly the opposite, predominantly increasing the analogous V1−O4 distance (1.913(4) Å; $\Delta_d = 0.100$ Å) and decreasing the apical V1−O1 distance (1.958(3) Å; $\Delta_d = -0.039$ Å) as well as the V1−O2 and V1−O3 distances ($\Delta_d = -0.025$ Å, -0.030 Å). However, the most significant change for both V1/V2 is across the shared O4 vertex that forms the rung of the spin ladders. Calculated bond valence sums[18] for each V coordination environment show a clear differentiation and give +4.21 for V1 and +4.99 for V2. Above the transition temperature, the sum of the bond valences for the single symmetry-unique V site is +4.47, as also found in the Co(pyz)-V_4O_{10} structure. Thus, the spin-gapped state is coupled to a charge disproportionation on vanadium that can roughly be written as $2V^{4.5+} \rightarrow V^{4+} + V^{5+}$, as shown in Figure 3A.

The antiferromagnetic spin-exchange interactions (J_{af}), and their dependence upon the underlying vanadate connectivity, have been probed using the spin-dimer analysis ($J_{af} \propto \Delta e^2$) as described and applied to layered vanadates before.[16,19] Prior results have shown there is one unpaired spin per O4 vertex-shared VO_5 pair, drawn in Figure 3 (top), that forms the ladder "rung". The apexes of the shared VO_5 pyramids alternate in an "up−down" pattern down the chain. The electronic structure analyses show the largest antiferromagnetic exchange interactions occur between the rungs of the ladder, giving a spin-ladder topology. Below the transition temperature, a charge ordering occurs both down these ladders and between neighboring ladders in a super-antiferroelectric pattern, as illustrated in Figure 3A (bottom). Analyses of the possible labeled pathways (Δe_x; x labeled as 1, 2, and 3) for superexchange for the charge-localized electrons yield a topology of spin-alignment as drawn. Here, the superexchange interactions between V^{4+} spins on neighboring rungs down chain ($\Delta e_1 = 134$ meV) and edge-shared V^{4+} pairs ($\Delta e_2 = 97$ meV) are much larger than that between every other spin site down the chain ($\Delta e_3 = 16$ meV). Thus, the antiferroelectric ordering both down and between ladders demonstrates a new charge-ordered structure that also couples to the predominant spin-exchange pathways and is labeled spin-superantiferroelectric II.

Several new and general insights regarding the origins of this new type of phase transition emerge via structural comparisons to the vanadate layers in ά-NaV_2O_5, which undergo a spin-SAF transition. The spin ladders in ά-NaV_2O_5, shown in Figure 3B, are similarly constructed from vertex-shared VO_5 pyramids, but with all apical O atoms oriented in the same direction. This structure results in antiferromagnetic exchange interactions to neighboring ladders that are equivalent ($J_a = J_b$). Thus, while a zigzag pattern of charge localization occurs down individual ladders, to neighboring ladders there are multiple degenerate interactions. This helps lead to the multiple superstructures, one of which is shown in Figure 3B (bottom). However, in $M(pyz)V_4O_{10}$, the apical oxygen atoms alternate in an "up−down" pattern owing to the coordination by M to every other pair (Figure 2A). This new layered structure yields nonequivalent interactions between neighboring ladders, with apical O atoms either on the same (J_a) or opposite (J_b) side of the layer, with $J_a > J_b$ by a factor of 4 or more. In this case, the possibility of multiple superstructures is decreased, along with the formation of a new spin-SAF II structure. Further, the incorporation of Co-$(pyz)^{2+}$ chains that order antiferromagnetically suppresses the transition by frustrating the spin alignment on the vanadate ladder.

The $M(pyz)V_4O_{10}$ hybrids demonstrate the use of metal-organic layers in tuning vanadate layer structures and which we here show can provide general new insights into the origins of magnetic phase transitions. These examples present many further theoretical opportunities and challenges, and that will be the source of future insights into strongly correlated electron systems.

Acknowledgment. Support provided from the National Science Foundation (DMR-0644833), Beckman Foundation via the Beckman Young Investigator program (to P.M.), and to Antoine Villesuzanne for help with low-temperature data for M = Co.

Supporting Information Available: Complete X-ray crystallographic data in CIF format is provided for each hybrid solid. This material is available free of charge via the Internet at http://pubs.acs.org.

References

(1) Lemmens, P.; Millet, P. *Lect. Notes Phys.* **2004**, *645*, 433−477.
(2) Ueda, Y. *Chem. Mater.* **1998**, *10*, 2653−2664.
(3) Chirayil, T.; Zavalij, P. Y.; Whittingham, M. S. *Chem. Mater.* **1998**, *10*, 2629−2639.
(4) Kanada, M.; Harashina, H.; Tanaka, S.; Fukamachi, T.; Kobayashi, Y.; Sato, M. *J. Phys. Soc. Jpn.* **1998**, *67*, 2904−2909.
(5) Zhang, Y.; DeBord, J. R. D.; O'Connor, C. J.; Haushalter, R. C.; Clearfield, A.; Zubieta, J. *Angew. Chem., Int. Ed. Engl.* **1996**, *35*, 989−991.
(6) Nazar, L. F.; Koene, B. E.; Britten, J. F. *Chem. Mater.* **1996**, *8*, 327−329.
(7) Isobe, M.; Ueda, Y. *J. Phys. Soc. Jpn.* **1996**, *65*, 1178−1181.
(8) Fujii, Y.; Nakao, H.; Yosihama, T.; Nishi, M.; Nakajima, K.; Kakurai, K.; Isobe, M.; Ueda, Y.; Sawa, H. *J. Phys. Soc. Jpn.* **1997**, *66*, 326−329.
(9) Chitov, G. Y.; Gros, C. *J. Phys.: Condens. Matter* **2004**, *16*, L415−L420.
(10) Joly, Y.; Grenier, S.; Lorenzo, J. E. *Phys. Rev. B* **2003**, *68*, 104412.
(11) Ohwada, K.; Fujii, Y.; Katsuki, Y.; Muraoka, J.; Nakao, H.; Murakami, Y.; Sawa, H.; Ninomiya, E.; Isobe, M.; Ueda, Y. *Phys. Rev. Lett.* **2005**, *94*, 106401.
(12) Gros, C.; Chitov, G. Y. *Europhys. Lett.* **2005**, *69*, 447−453.
(13) Ohta, Y.; Nakaegawa, T.; Ejima, S. *Phys. Rev. B* **2006**, *73*, 045101.
(14) Edegger, B.; Evertz, H. G.; Noack, R. M. *Phys. Rev. Lett.* **2006**, *96*, 146401.
(15) Ohwada, K.; Fujii, Y.; Nakao, H.; Murakami, Y.; Isobe, M.; Ueda, Y. *Mod. Phys. Lett. B* **2006**, *20*, 199−214.
(16) Yan, B.; Luo, J.; Dube, P.; Sefat, A. S.; Greedan, J. E.; Maggard, P. A. *Inorg. Chem.* **2006**, *45*, 5109−5118.
(17) Additional refinement data for $M(pyz)V_4O_{10}$: M = Co, $T = 12$ K, crystal dimensions = 0.2 × 0.2 × 0.05 mm, 1036 reflections, 64 parameters, $R1/wR$ = 0.033/0.079, GOF = 1.34; M = Zn, $T = 10$ K, crystal dimensions = 0.33 × 0.12 × 0.02, 2153 reflections, 96 parameters, $R1/wR2$ = 0.035/0.094, GOF = 1.11, Flack parameter = 0.48(3) (racemic twin). See Supporting Information.
(18) (a) Brown, I. D.; Altermatt, D. *Acta Crystallogr.* **1985**, *B41*, 244. (b) Brese, N. E.; O'Keefe, M. *Acta Crystallogr.* **1991**, *B47*, 192.
(19) Whangbo, M. H.; Koo, H.-J.; Lee, K.-S. *Solid State Commun.* **2000**, *114*, 27−32.

JA0754709